JOURNAL OF MATERIALS SCIENCE 27 (1992) 5375–5381

Non-linear properties of metallic cellular materials with a negative Poisson's ratio

J. B. CHOI, R. S. LAKES*
*Department of Biomedical Engineering, *and also Department of Mechanical Engineering, and the Center for Laser Science and Engineering, University of Iowa, Iowa City, IA 52242, USA*

Negative Poisson's ratio copper foam was prepared and characterized experimentally. The transformation into re-entrant foam was accomplished by applying sequential permanent compressions above the yield point to achieve a triaxial compression. The Poisson's ratio of the re-entrant foam depended on strain and attained a relative minimum at strains near zero. Poisson's ratio as small as -0.8 was achieved. The strain dependence of properties occurred over a narrower range of strain than in the polymer foams studied earlier. Annealing of the foam resulted in a slightly greater magnitude of negative Poisson's ratio and greater toughness at the expense of a decrease in the Young's modulus.

1. Introduction

Cellular solids are lightweight materials consisting of a network of solid ribs or plates. Man-made cellular solids have been widely utilized in the form of structural honeycombs (two-dimensional cellular solids) in aircraft and in the form of foams (three-dimensional cellular solids) for packing, cushioning, energy-absorption applications, sandwich panel cores, structural purposes and thermal protection systems. Natural materials such as wood, cancellous bone, coral and leaves have a cellular structure. All these "conventional" cellular materials have a convex cell shape and exhibit a positive Poisson's ratio. Recently, isotropic foam structures with negative Poisson's ratios have been fabricated by one of the authors [1]. The fabrication was achieved through a transformation of the cell structure from a convex polyhedral shape to a concave or "re-entrant" shape. Increase in some material properties such as flexural rigidity and plane strain fracture toughness was predicted [1–3].

The range of Poisson's ratio for isotropic material is -1 to 0.5, as demonstrated by energy arguments [4]. Negative Poisson's ratios are rare but not unknown. Negative Poisson's ratios have been reported in single-crystal pyrites [5] and in some rocks [6]. Synthetic anisotropic microstructures [7] were found to give such an effect. One of the authors [8] suggested that, in the absence of pre-strain, non-affine deformation kinematics are essential for the production of negative Poisson's ratios in isotropic materials. A recent study of polymeric re-entrant foams with negative Poisson's ratio [9] reported other enhanced material properties: an increase in the toughness, in the shear modulus and in the resilience in the sense of a wide range of linear stress–strain behaviour. Conventional and re-entrant polymer foams also differ in their stress–strain behaviour and deformation mechanism maps [9]. In copper foam an increase in the indentation resistance with re-entrant transformation was demonstrated experimentally [10], which is consistent with theory [11].

Mechanical properties of a conventional foam material depend on the physical properties of the solid material making up the cell ribs, relative density (the ratio of the bulk density of the foam material to the density of the solid from which it is made), cell shape, cell size and loading conditions. The simplest and most comprehensive treatment of conventional foam properties is that of Gibson and Ashby [12], which includes extensive comparisons between analytical results and experiment. In re-entrant foam, relative density is increased and the cell size is reduced slightly by the transformation process; the cell shape is dramatically altered. Mechanical behaviour of a re-entrant foam material differs from that of a conventional foam in ways not addressed by existing theoretical treatments; most of the difference is attributed to the change in cell shape.

In this study, the mechanical properties of both conventional and re-entrant copper foam materials are examined at small strain by optical methods and at larger strains by servohydraulic (MTS) machine tests.

2. Experimental procedure

2.1. Specimen preparation: optical study

A large block of copper foam with relative density between 0.08 and 0.1 was cut into smaller 18 mm $\times$ 18 mm $\times$ 36 mm blocks; another large block with relative density 0.04 was cut into 25 mm $\times$ 25 mm $\times$ 50 mm blocks. Bar-shaped specimens were cut from these blocks using the procedure described below. The blocks were not perfectly uniform: specimens of relative density of 0.04, 0.08, 0.09, 0.1 had deviations of 12%, 6%, 5.5%, 5%, respectively, in relative density.

0022–2461

Block specimens were cut with a high-speed saw to minimize surface plastic deformation. The foam was then transformed into a re-entrant structure by applying small sequential increments (less than 2% strain) of plastic deformation in three orthogonal directions using a vise fitted with PMMA (Plexiglas®) end pieces to provide an even surface. The compressed foams were cut again into slender bars (approximately 7 mm × 7 mm × 30 mm) following the above cutting method. The lengths of the cell ribs were measured with a microscope in order to compare the cell size for each specimen.

The re-entrant foam specimens have irregular surfaces which were polished with graded abrasives (silicon carbide grits 120, 320, 600 and 1000), under water irrigation, in order to obtain a smooth surface for optical tests. The water irrigation served to minimize temperature increases due to friction and improved the surface finish. High grinding speed and low pressure were used to avoid plastic deformation of the surface. The finest polishing medium grains of 1000 mesh had a size of about 18 μm [13]. This provided sufficient smoothness to the surface so that the shadow Moiré method could be applied to measure deformation.

2.2. Specimen preparation – MTS machine test

Rectangular specimens from a large block of initial relative density 0.08 ± 5%, were made with volumetric compression ratio of 1, 2.0, 2.5, 3.0, according to the ASTM standard for subsize specimens [14] for both tension and compression tests. The dimensions of the specimens were 6.4 mm × 6.4 mm × 25.4 mm for tension, 19 mm × 19 mm × 9.5 mm for compression; the compression specimens were made shorter to prevent buckling. These specimens were polished as described above.

Specimen ends were cast in dental grade polymethyl methacrylate (PMMA) which is much more rigid ($E \approx 3$ GPa) than the copper foam ($E \approx 200$ MPa). This procedure avoided the machine grips crushing the ends. The mould for casting was threaded and was made of Teflon® and was sprayed with Teflon® lubricant to prevent adhesion of the polymerizing PMMA. The viscosity of the polymerizing PMMA was adjusted to minimize leakage from the mould and to be sufficiently low to mould adequate threads. The curing temperature of PMMA was about 80 °C, too low to affect the material properties of the copper foam.

2.3. Annealing

The re-entrant copper foam has some cold work due to the tri-axial compressions, so an annealing process was used to evaluate the effects of cold work. The polished specimen was dried for 2 days in room conditions and heated under nitrogen purge at a temperature of 500 °C for 1 h [15] and cooled slowly under nitrogen to minimize oxidation.

2.4. Optical test – shadow Moiré

The Moiré methods are based on fringe patterns arising from overlap between gratings consisting of straight parallel opaque bars. In the shadow Moiré method, a Ronchi ruling is placed close to the specimen surface and is illuminated with collimated light. Overlap occurs between the ruling and its reflected (shadow) image, generating fringes which represent a contour map of the deformed surface. The displacement, δ, of the surface perpendicular to itself is given by [16]

$$\delta = Np/(\tan\alpha + \tan\beta) \quad (1)$$

where N is the fringe order, p is the pitch of the grating, α is angle of the incident light and β is the viewing angle with respect to the normal to the grating.

Specimens of initial relative densities of 0.08, 0.09 and 0.1 were used; however, conventional foam of initial relative density of 0.04 was not used in the optical test because of the poor fringe pattern due to the large cell size.

Bending experiments were performed by applying known weights to an aluminium arm cemented to the top end of a vertically oriented copper foam specimen; the lower end was clamped. The aluminium arm was sufficiently long that specimen strain due to bending substantially exceeded compressional strain, approximating "pure" bending. The Young's modulus, E, and Poisson's ratio, ν, were extracted from the displacement field by first using simple beam theory to obtain an approximate value for E from the end deflection, δ

$$\delta = ML^2/2EI \quad (2)$$

where M is the bending moment, L is length, and I is the area moment of inertia. Then the three-dimensional solution was used to infer ν and obtain a corrected value for E

$$\delta = ML^2(z^2 + \nu x^2 - \nu y^2)/2EI \quad (3)$$

in which z is a longitudinal co-ordinate along the length of the bar, x is a lateral co-ordinate, and y is a transverse co-ordinate. The correction to E was small in all cases. Positive Poisson's ratios give rise to hyperbolic fringe contours, and negative Poisson's ratios give rise to elliptic contours. In either case the Poisson's ratio was found from the observed shape of the contours.

In this experiment, the grating was located a small distance, within a millimetre, away from the specimen, parallel to the surface and oriented so that no fringe pattern occurred. Light from a mercury vapour lamp was collimated by a lens and directed upon the grating at an angle 48° from the normal to the grating plane; the viewing angle was 19°. A 300 line/in (11.8 line/mm) grating was used for determining the elastic modulus and a 1000 line/in (39.4 line/mm) grating for obtaining the Poisson's ratio, because the latter was too sensitive for ready determination of fringe order at the specimen end. For Poisson's ratio determination, the grating was tilted so that the centre of the fringe pattern appeared near the centre of the bar. Measurements were performed at a specimen surface strain of

0.05%–0.1%. Theoretical contour lines based on Equation 3, prepared for a variety of Poisson's ratio were drawn with an Apollo computer using "Promatlab" graphics software to facilitate the analysis of the observed fringe patterns appearing on the specimen surface.

2.5. MTS machine test

A servohydraulic testing machine (MTS corp) with a 2.5 kN load cell was used to apply loads for the characterization of non-linear properties of the foams. All the experiments were performed at equal strain rates of 0.006 s^{-1}. To determine lateral deformation for the purpose of determining Poisson's ratio, dial gauges (no. 25-109, Starrett company, resolution 1.2 μm, range 0.38 mm) were applied to each lateral surface near the centre portion of the specimen. A flat tip was used in contact with the specimen in the case of lateral bulging, while a round one was used to evaluate lateral contraction. A universal joint was used in the tension test and a small ball socket joint was used in the compression test to ensure alignment. In compression tests, Teflon tape was used between the specimen and the loading surface to minimize the friction force on the contact surfaces.

3. Results and discussion

In the conventional copper foam, the Moiré fringe patterns were observed to be hyperbolas corresponding to a positive Poisson's ratio. Accuracy in the Poisson's ratio determination was limited to ± 0.1 by uncertainty (about ± 5%) in measuring the slope of the asymptote. For homogeneous materials, accuracy could be improved by increasing the strain hence the fringe density; however, in these materials the fringes became blurred beyond a certain strain [17]. In the re-entrant copper foams, the Moiré fringes had elliptical contours corresponding to a negative Poisson's ratio. It was possible to achieve better accuracy in this case as a result of the different fringe shape and the greater compliance of the transformed material.

Figs 1 and 2 show optically determined Poisson's ratio at small strain as it depends on the initial and final relative densities. The Poisson's ratio of conventional foam with initial relative density of 0.09 is 0.2 ± 0.1. In the re-entrant foam, the smallest Poisson's ratio observed was − 0.8 ± 0.05 at a strain of 0.1%; the permanent volumetric compression ratio was 2.13 and the initial relative density was 0.1.

The negative Poisson's ratio of re-entrant foam attains a minimum for an optimal value of permanent volumetric compression ratio; the optimal compression is smaller for higher values of initial relative density, as shown in Fig. 1. For copper foam with initial relative density of 0.04 the optimal compression ratio, 3.6, is comparable to that of the polymer foams, 3.3–3.7, which have a similar relative density of 0.03. This correspondence between two different materials suggests a geometrical cause associated with the cell structure. In particular, the optimum volumetric compression ratio arises in part from the fact that too much compression causes the ribs to come in contact, which hinders the unfolding which gives rise to the negative Poisson's ratio. One would naively expect the optimum to occur for a particular final relative density (determined as the product of the initial relative density and the volumetric compression ratio). Fig. 2, however, shows the optimum to depend on both the initial and final relative densities, so the above interpretation is incomplete.

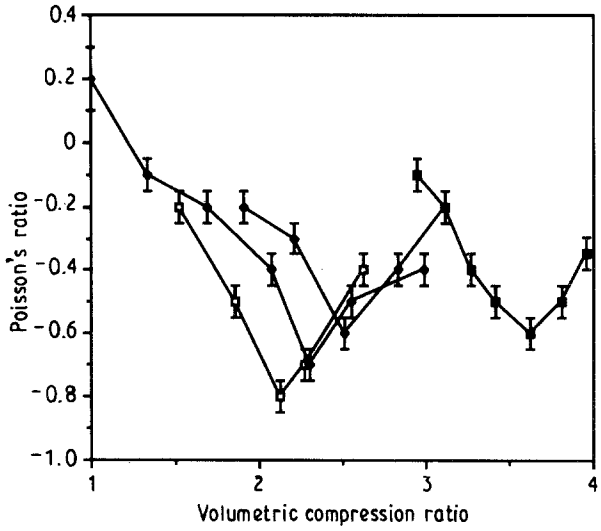

Figure 1 Poisson's ratio versus volumetric compression ratio. Initial relative density: (□) 0.1, (◇) 0.09, (◆) 0.08, (■) 0.04.

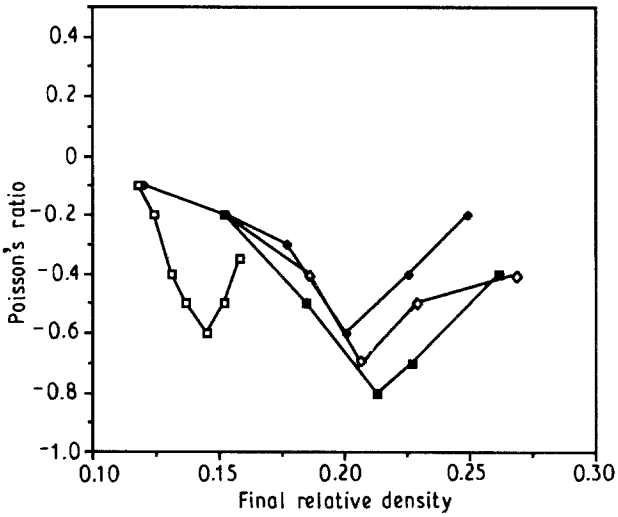

Figure 2 Poisson's ratio versus final relative density. Initial relative density: (■) 0.1, (◇) 0.09, (◆) 0.08, (□) 0.04.

The elastic modulus decreases monotonically with permanent volumetric compression as shown in Fig. 3, so that re-entrant copper foam is less stiff than the conventional foam from which it was derived. Polymer foams behaved similarly, except that for sufficiently large permanent volumetric compression, the stiffness began to increase again.

The effect of annealing on the relationships between stress and engineering strain for foams with volumetric compression ratios of 1, 2.0, 2.5, 3.0 is shown in Fig. 4. In tension, most of the specimens failed near the cast polymer end piece due to stress concentration; the

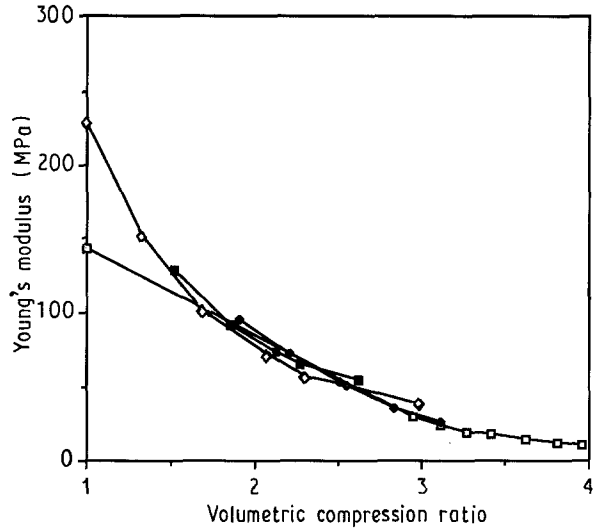

Figure 3 Dependence of Young's modulus on initial relative density and upon volumetric compression ratio. Initial relative density: (■) 0.1, (◇) 0.09, (◆) 0.08, (□) 0.04.

end points on the tensile side of the graphs represent this fracture. In compression, the tests were terminated at the beginning of unstable compression due to buckling. The conventional foam has some strain-hardening tendency, but the re-entrant foam does not exhibit this effect, thus, the latter can be modelled as an elastic–perfectly plastic material. In both tension and compression, the conventional and re-entrant foams exhibit a rather long plateau above the proportional limit. This behaviour is attributed to the plastic hinge formation of cell ribs which occurs when the moment exerted on the cell ribs equals or exceeds the fully plastic moment. By contrast, the fracture behaviour of both conventional and re-entrant copper foam in tension was brittle-like: failure occurred abruptly without necking or drawing. The foams were brittle even though the solid copper from which the foam was made is ductile; similar behaviour has been observed in other foams and has been analysed in view of the alignment of cell ribs which occurs under tension [12].

In the compressive properties, errors can arise due to the effect of friction with the loading surface combined with the Poisson effect. An apparent yield stress, $\sigma_{y,app}$, can be expressed [18] in terms of the true yield stress for a specimen with a ratio of 2:1 in width to height as $\sigma_{y,app} = \sigma_{y,true}(1 + m)$, where m is the friction coefficient. Because m is less than 0.1 for copper and Teflon, the maximum experimental deviation through the whole load history due to the friction force is within 10%.

For the conventional copper foams the properties in tension and compression are similar, as seen in Fig. 4. Young's modulus and the ultimate strength are lower by about 33% and 25%, respectively, for annealed material. The inset graph shows that the foams are non-linear even for strains below 1%; by contrast to the polymer foams studied earlier. The difference arises from the yield of the ribs in copper foam at small strain. The re-entrant specimens as shown in Fig. 4 show very dissimilar properties in tension and compression. Increase in the permanent volumetric compression ratio results in reduced tensile stiffness and increased compressive stiffness, as seen in Fig. 5 which shows the effective Young's modulus at 0.5% strain as it depends upon permanent volumetric compression

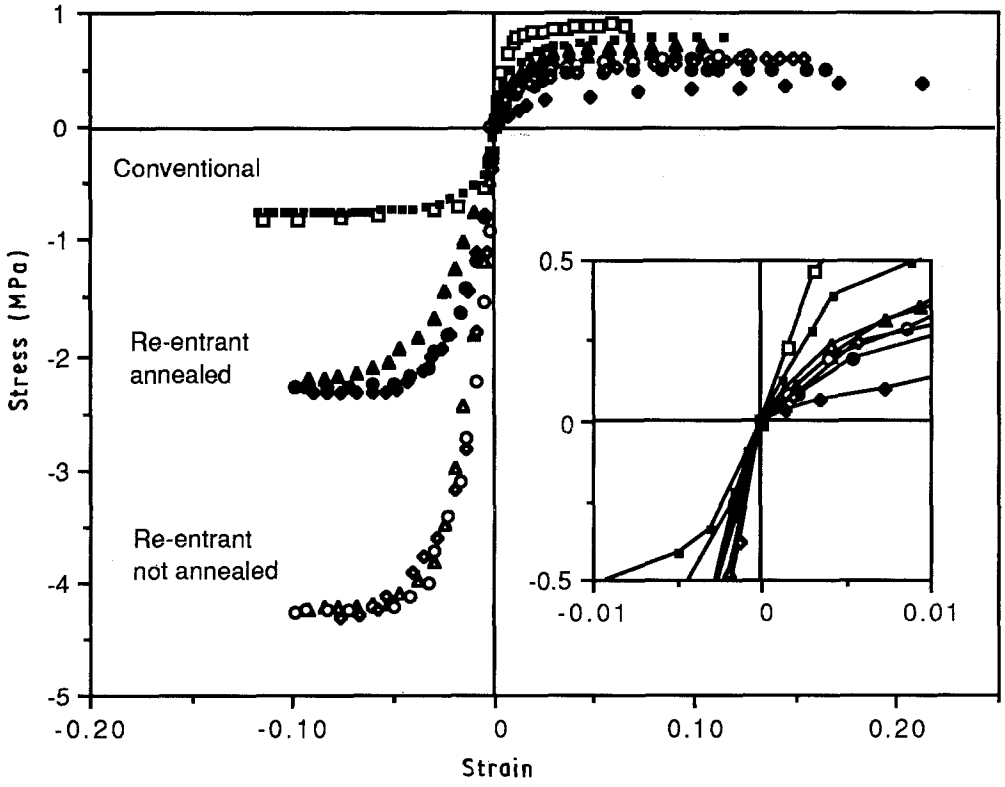

Figure 4 Stress–strain relationships for conventional and re-entrant foams. Initial relative density 0.08. (■, ▲, ●, ◆) Annealed, (□, △, ○, ◇) not annealed. (■, □) Conventional foam, volumetric compression 1. (▲, △) Re-entrant foam, volumetric compression 2.0. (●, ○) Re-entrant foam, volumetric compression 2.5. (◆, ◇) Re-entrant foam, volumetric compression 3.0.

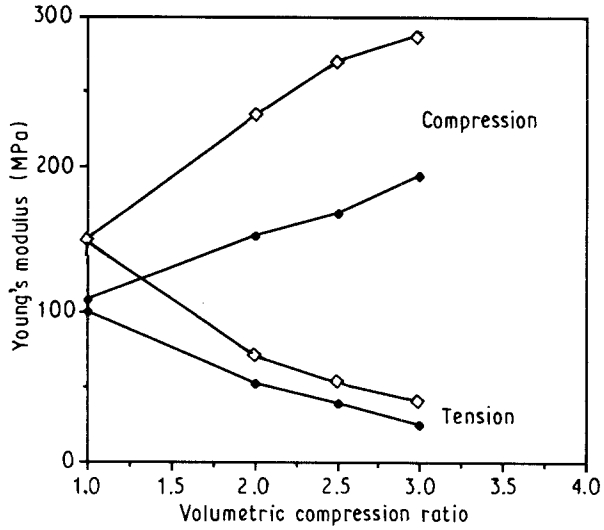

Figure 5 Young's modulus versus permanent volumetric compression ratio for (◆) annealed and (◇) non-annealed copper foam at a strain of 0.5%.

ratio. As for ultimate strength, it is reduced by about 15% in both tension and compression by the annealing process.

The 0.2% offset yield strength and yield strain of the conventional copper foam appeared to be nearly the same in tension and compression as shown in Table I. However, the yield strength of re-entrant foam decreased in tension with the volumetric compression ratio, and increased in compression. The decrease in the yield strength of the re-entrant foam in tension is attributed to the weakness of the plastic hinges formed in the cell ribs during the permanent volumetric compression. The increase in the yield strength in compression is attributed to the contact of some of the cell ribs with each other during compression. Annealing effects provoked a decrease in the yield strength and an increase in the yield strain. Plastic collapse can occur in foams made of a ductile solid when the moment exerted on the cell ribs exceeds the fully plastic moment, forming plastic hinges. The plastic collapse stress or the yield strength was given as $\sigma_y = 0.3\sigma_{ys}(\rho^*/\rho_s)^{1.5}$, in which ρ_s and σ_{ys} is the density and yield strength of the solid from which the foam was made, respectively, and ρ^* is the bulk density of the foam material [12]. The properties of solid copper were taken as $\rho_s = 8.9\,g\,cm^{-3}$ and $\sigma_{ys} = 60$ MPa [12]. The yield strength of the conventional copper foam was predicted to be 0.42 MPa. The yield strength of the conventional copper foam was found to be 0.65 MPa in tension, 0.58 MPa in compression from MTS machine test as shown in Table I. The agreement is satisfactory in that the experimental result represents the 0.2% yield strength.

The tension experiments disclosed that the toughness, defined as the energy per unit volume to fracture, of the re-entrant foam compared to that of conventional foam, increased by factors of 1.4, 1.5, 1.7 with increases of volumetric compression ratio of 2.0, 2.5, 3.0, respectively. Annealing effects can further increase the toughness. This effect was most evident at a volumetric compression ratio of 2.0, as shown in Fig. 6. However, the annealed re-entrant foams at a volumetric compression ratio of 2.5 did not show as much increase, and the toughness actually decreased in the foam at a volumetric compression ratio of 3.0. In the case of an elastomeric foam such as polyurethane foam, the experimental results showed increases by factors of 1.7, 2.1, 2.3, 2.6, 3.2 in the toughness of the re-entrant foam compared to that of the conventional foam, at volumetric compression ratios of 2.0, 2.6, 3.2, 3.7, 4.2, respectively [9]. Elastomeric foam (which can be deformed at large strain) exhibited a somewhat greater toughness increase with re-entrant transformation in comparison to copper foam (which is elasto-plastic).

The Poisson's ratio of the conventional foam shows highly non-linear dependence upon the engineering strain, as shown in Fig. 7. The Poisson's ratios of the conventional copper foam are near 0.35 for small strain and approach 0.5 in tension and 0 in compression; similar behaviour was observed in conventional polymer foam [9]. This approach of Poisson's ratio to zero at large strain in compression also agrees with other results: Poisson's ratio for the plastic compression of foam material was typically 0.03–0.05 [19, 20] and Poisson's ratio beyond the yield point was 0.04 [21] in compression.

In the theoretical study of small-strain behaviour of conventional foam, a strong dependence of Poisson's ratio on the bulk density at a strain of not more than 0.5% was suggested [22]. Other authors showed a constant Poisson's ratio of 0.33 [12, 23, 24] or 0.23 [25] independent of relative density. Even though the cell morphology changes with the relative density [25], any effect may be difficult to extract from the considerable scatter in experimental values for Poisson's ratio [12]. The density changes in the re-entrant foam are accompanied by cell shape changes, so the above considerations are not applicable.

Annealed specimens gave a slightly better negative effect in the Poisson's ratio (Figs 7–9) at the expense of a decrease in the Young's modulus for each volumetric

TABLE I 0.2% offset yield strength and strain of the conventional and re-entrant copper foam. The values in parentheses are the yield strains (%)

Volumetric compression ratio	σ_y (MPa) (% strain)			
	Tension	Compression	Tension	Compression
1.0	0.65 (0.64)	0.58 (0.60)	0.45 (0.67)	0.43 (0.63)
2.0	0.28 (0.62)	1.83 (0.97)	0.33 (0.85)	1.24 (1.16)
2.5	0.26 (0.74)	2.34 (1.08)	0.23 (0.81)	1.23 (0.92)
3.0	0.28 (0.87)	2.37 (1.10)	0.14 (0.95)	1.06 (0.80)

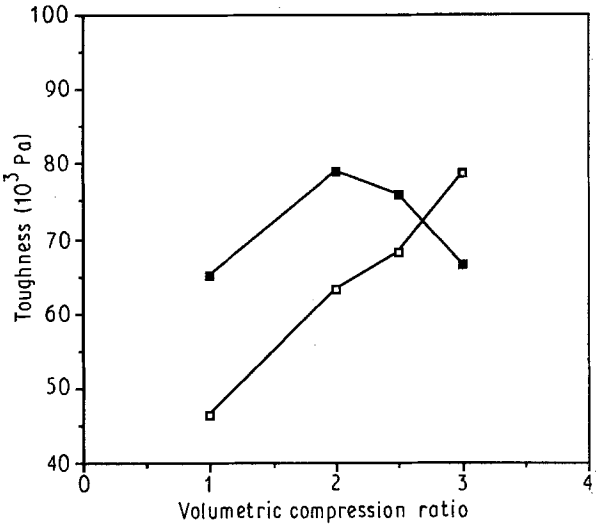

Figure 6 Toughness versus permanent volumetric compression of the conventional and re-entrant copper foams: (□) non-annealed, (■) annealed.

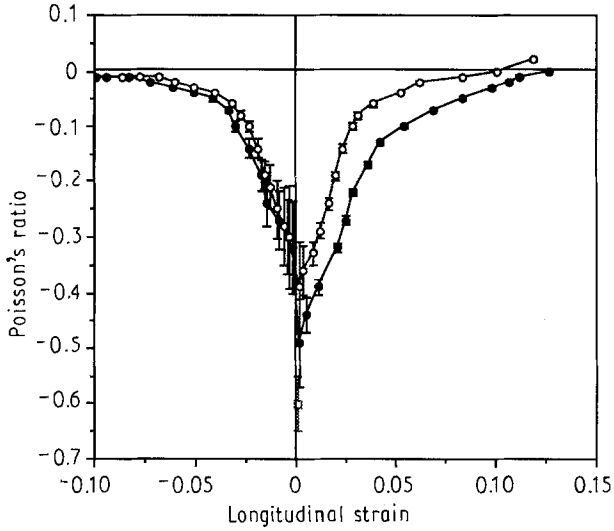

Figure 8 Poisson's ratio versus longitudinal strain for volumetric compression ratio of 2.5. Initial relative density 0.08. (○) Non-annealed, (●) annealed, (□) optical results.

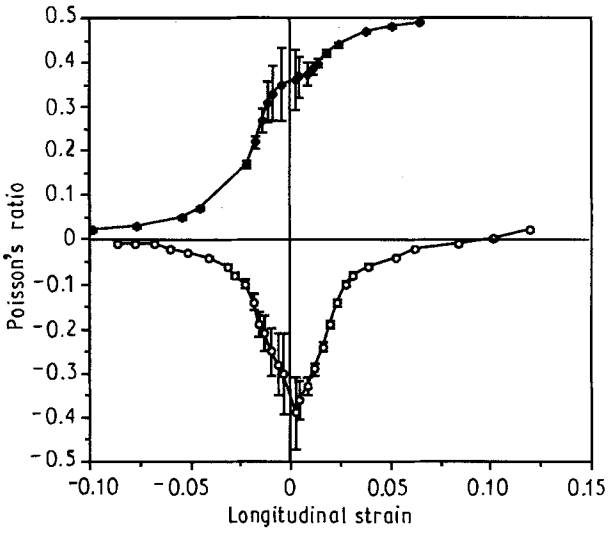

Figure 7 Poisson's ratio versus longitudinal strain for copper foam. Initial relative density: 0.08. (◆) Conventional foam, (○) re-entrant foam, not annealed, volumetric compression ratio of 2.0.

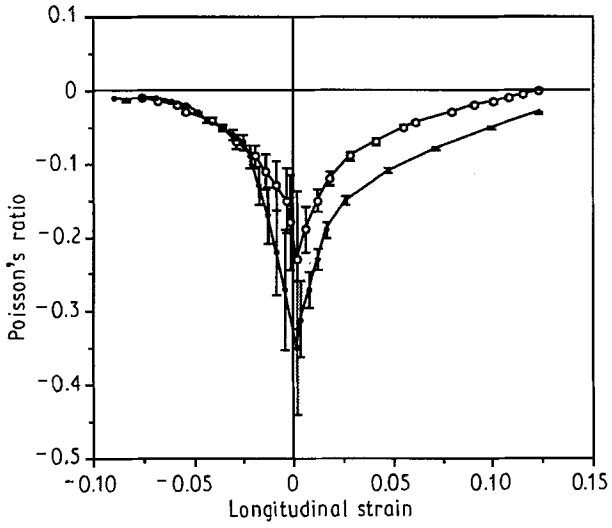

Figure 9 Poisson's ratio versus longitudinal strain for volumetric compression ratio of 3.0. Initial relative density 0.08. (○) Non-annealed, (●) annealed.

compression ratio. The lowest Poisson's ratio obtained in this mechanical testing (MTS) experiment was -0.49 at a strain of 0.2% as indicated in Fig. 8. In comparison, a Poisson's ratio of -0.6 ± 0.05 was determined optically at a strain of 0.1% for specimens having the same initial relative density of 0.08 and the same volumetric compression ratio of 2.5. A minimum Poisson's ratio of -0.8 ± 0.05 was determined optically at a strain of 0.1% for a different specimen as described above. Friis *et al.* [3] obtained a minimum Poisson's ratio of -0.39 at a compressive strain of 0.013 in mechanical tests on copper foam with a permanent volumetric compression ratio of 2.0 and a relative density of 0.053. The difference may be attributed to the highly non-linear behaviour of the metal foam as indicated by the cusp in Poisson's ratio versus strain curves. This contrasts with the polymeric foam which exhibited a smoother dependence of Poisson's ratio upon strain and which exhibited a broader minimum in Poisson's ratio versus strain curves, in comparison with the metal foams. The difference in behaviour between the metal and polymer foams is attributed to the fact that the ribs of the copper foam can yield and form plastic hinges at relatively small strain, in contrast to the polymer which is an elastomer. The non-linearities in compression are attributed in part to regions of contact between cell ribs in the re-entrant foam; no such contacts occur in the conventional foam (Fig. 10). The deformation mechanism map of copper foams (Fig. 11) differs from that of the polymer foams in that the linear elastic range occurs over a narrower region of strain than in polymer foam. Moreover, tension causes a reduction of apparent stiffness due to yield, in contrast to the polymer foams which attain such large strains that the ribs become oriented.

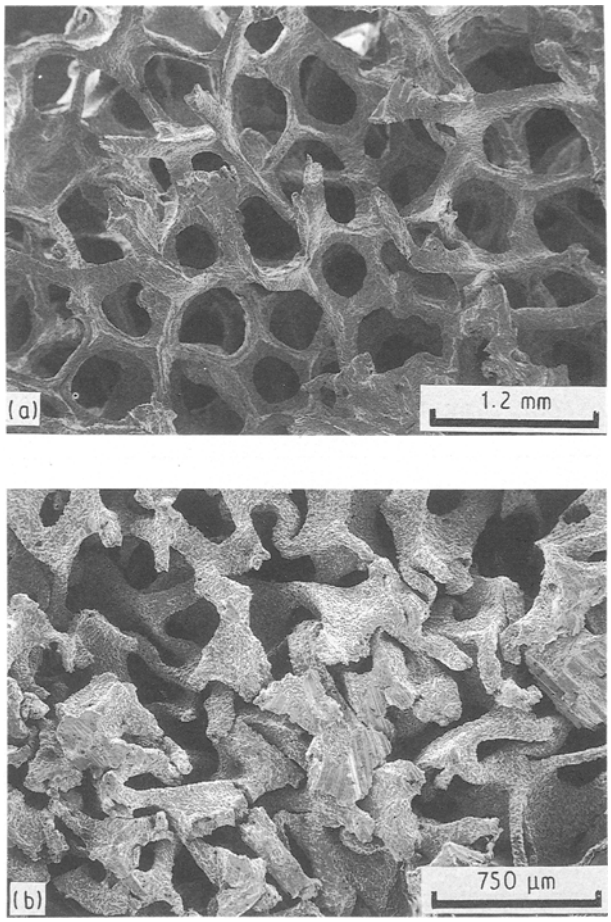

Figure 10 Scanning electron micrographs of (a) conventional copper foam, relative density 0.08, and (b) re-entrant copper foam, initial relative density 0.03, volumetric compression ratio 2.5.

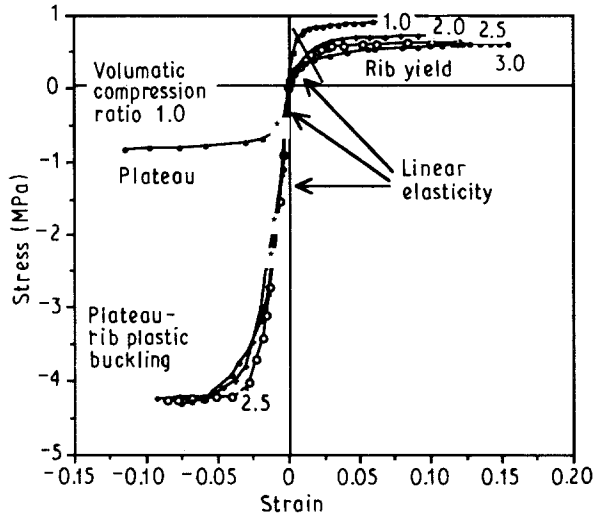

Figure 11 Deformation mechanism map for copper foams of various permanent volumetric compression ratios.

4. Conclusions

1. The Poisson's ratio of both conventional and re-entrant foam depends on strain. Poisson's ratio of re-entrant foam attains a relative minimum as small as − 0.8 for zero strain.

2. Optimum permanent compression to achieve the best negative Poisson's ratio depends on the initial foam relative density: higher density foam requires less compression for transformation. This optimum appears to have a purely geometrical origin, because the same value was observed for metal and polymer foam of the same relative density.

3. The re-entrant copper foam in compression does not exhibit strain hardening.

4. The toughness of the re-entrant foam increases with volumetric compression ratio and annealing effects further increase the toughness.

Acknowledgements

Support of this research by the NSF and by the NASA/Boeing ATCAS program under contract no NAS1-18889, and by a University Faculty Scholar Award (to R. S. L.) is gratefully acknowledged.

References

1. R. S. LAKES, *Science* **235** (1987) 1038.
2. *Idem, ibid.* **238** (1987) 551.
3. E. A. FRIIS, R. S. LAKES and J. B. PARK, *J. Mater. Sci.* **23** (1988) 4406.
4. Y. C. FUNG, "Foundation of Solid Mechanics" (Prentice-Hall Englewood, NJ, 1968) p. 353.
5. A. E. H. LOVE, "A Treatise on the Mathematical Theory of Elasticity" (Dover, New York, 1944) p. 163.
6. O. G. INGLES, I. K. LEE, R. C. NEIL, *Rock Mech.* **5** (1973) 203.
7. K. E. EVANS, B. CADDOCK, *J. Phys. D Appl. Phys.* **22** (1989) 1883.
8. R. S. LAKES, *J. Mater. Sci.* **26** (1991) 2287.
9. J. B. CHOI and R. S. LAKES, *ibid.*
10. K. ELMS and R. S. LAKES, in preparation.
11. S. P. TIMOSHENKO and J. N. GOODIER, "Theory of Elasticity" (McGraw-Hill, New York, 1969).
12. L. J. GIBSON, M. F. ASHBY, "Cellular Solids" (Pergamon Press, Oxford, 1988).
13. L. E. SAMUELS, "Metallographic Polishing by Mechanical Methods" (American Society for Metals, Metals Park, OH, 1982) pp 80–1.
14. "Annual Book of ASTM Standards", Designation: E8-85b (American Society for Testing and Materials, Philadelphia, PA, 1986).
15. "Metal Handbook, Heat Treating, Cleaning and Finishing" (American Society for Metals, Metals Park, OH) p. 285.
16. A. S. KOBAYASHI, "Manual of Engineering Stress Analysis" (Prentice Hall, Cambridge, 1982) pp 62–3.
17. C. P. CHEN and R. S. LAKES, *J. Mater. Sci.* in press.
18. R. HILL, "The Mathematical Theory of Plasticity" (Oxford University Press, New York, 1983) p. 236.
19. M. C. SHAW and T. SATA, *Int. J. Mech. Sci.* **8** (1966) 469.
20. J. A. RINDE, *J. Appl. Polym. Sci.* **14** (1970) 1913.
21. M. WILSEA, K. L. JOHNSON and M. F. ASHBY, *Int. J. Mech. Sci.* **17** (1975) 457.
22. A. G. DEMENT'EV, P. I. SELIVERSTOV and O. G. TARAKANOV, *Mekhan. Polim.* **1** (1973) 45.
23. A. N. GENT and A. G. THOMAS, *Rubb. Chem. Tech.* **36** (1963) 597.
24. J. M. LEDERMAN, *J. Appl. Polym. Sci.* **15** (1971) 693.
25. A. McINTYRE and G. E. ANDERTON, *Polymer* **20** (1979) 247.

Received 6 August
and accepted 10 September 1991